

# Influence of Long-Chain Aliphatic Dopants on the Spectroscopic Properties of Polyketimine Containing 3,8-Diamino-6-phenylphenanthridine and Ethylene Linkage in the Main Chain. Noncovalent Interaction: Proton Transfer, Hydrogen and Halogen Bonding

Agnieszka Iwan,\* Bożena Kaczmarczyk, Bożena Jarzabek, Jan Jurusik, Marian Domanski, and Michał Michalak

Centre of Polymer and Carbon Materials, Polish Academy of Sciences, 34 M. Curie-Skłodowska Street, 41-819 Zabrze, Poland

Received: March 5, 2008; Revised Manuscript Received: May 8, 2008

The spectroscopic properties of the aromatic polyketimine containing 3,8-diamino-6-phenylphenanthridine and ethylene linkage in the main chain (PK1) before and after doping are dominated by an interplay of electron-donating and electron-withdrawing effects mediated by its nitrogen atom and active groups in the dopants, respectively. Hydrogen and halogen bond formation or molecular recognition between PK1 and decanoic acid (DCA), *n*-decyl alcohol (DA), 1,10-dibromodecane (DBr), and *n*-decyl sulfonic acid (DSA) was investigated in comparison with undoped PK1. UV–vis and Fourier transform infrared (FTIR) absorption, wide-angle X-ray diffraction (WAXD), and the atomic force microscopy (AFM) technique are used to probe the spectroscopic properties of the phenanthridine “core” of PK1 as well as its complexes. Spectral changes were observed for the PK1 after doping, which supported the ionic, hydrogen, and halogen bond formation between the PK1 and protonation agents (dopants). This specific interaction of the dopant with the host polymer influences the polyketimine properties, and the following changes were observed: (i) changes in the band gap ( $E_g$ ) of the protonated polyketimine, (ii) changes in the FTIR spectra of doped PK1, (iii) changes in optical micrographs of the protonated PK1 (detected by the AFM technique), and (iv) changes in crystalline structure of doped PK1. Our study demonstrates how the properties of conjugated PK1 can be tuned by the supramolecular engineering concepts, which could be important for optoelectronic applications of the materials.

## 1. Introduction

Intermolecular interactions play an important role in supramolecular chemistry and also crystal engineering.<sup>1</sup> The supramolecular chemistry, a term introduced by Jean-Marie Lehn, is chemistry beyond the molecule and is the chemistry of molecular assemblies using noncovalent bonds.<sup>2</sup> The noncovalent interactions are generally weak and vary from less than 5 kJ/mol for van der Waals forces, through approximately 50 kJ/mol for hydrogen bonds, to 250 kJ/mol for Coulomb interactions. Moreover, interactions between molecules can be analyzed on the basis of interactions between their structural atoms. Noncovalent phenomena such as  $\pi$ – $\pi$  stacking and hydrogen bonding have been studied extensively,<sup>3,4</sup> whereas so-called halogen bonding has received much less attention.<sup>5–9</sup> A hydrogen bond (B–HX) results when an electrophilic hydrogen atom  $H^{\delta+}$  of an acid (HX) interacts with a nucleophilic center on the Lewis base (B). In halogen bonding (B–XY) carbon-bound halogen atoms, usually Br or I, act as electron acceptors for the lone pair electrons of heteroatoms, i.e., O, N, S, or P.

The process of self-organization facilitates formation of ordered polymeric nanoscale structures and further allows elaboration of responsive materials. In the case of rodlike polymers (such as  $\pi$ -conjugated electroactive polymers) it could lead to possible new applications, but its use is not straightforward because such polymers tend to be infusible and poorly soluble.

The aromatic polyketimines (PKs), i.e., polymers containing C=N– groups in the main chain, being isoelectronic with the corresponding poly(*p*-phenylene-vinylenes (PPVs)), exhibit interesting electronic, luminescent, and nonlinear optical properties.<sup>10</sup> The principal feature of polyketimines which distinguishes them from the majority of conjugated polymers is the presence of basic centers in the polymer main chain associated with imine nitrogens. This implies that acid–base chemistry can be used for the modification of the polymer properties.<sup>10–15</sup> Polyketimines can be considered as a subclass of polyazomethines with a phenyl group attached to the methine carbon atom. Surprisingly, literature data concerning optical properties of polyketimines are rather scarce,<sup>10</sup> yet PKs seem to be excellent candidates for new polymeric luminescent materials because in addition to a rather facile tuning of their spectroscopic properties they should exhibit better thermal stability as compared to other luminescent polymers. The luminescence properties of polyketimines were investigated by Iwan and co-workers.<sup>10–14</sup>

In our previous paper we described the spectroscopic and optical properties, mainly photoluminescence, of undoped and doped polyketimines obtained from 3,8-diamino-6-phenylphenanthridine (DAPP) and three diketones, i.e., *p*-dibenzoylbenzene, dibenzyl, and *trans*-1,2-dibenzoylethylene.<sup>14</sup> The emission spectra of polymer obtained from 3,8-diamino-6-phenylphenanthridine and *trans*-1,2-dibenzoylethylene (abbreviated hereinafter as PK1) showed maximum at about 510 nm, under excitation wavelengths of 350 and 400 nm. The emission spectrum of the PK1 under an excitation wavelength of 450 nm exhibited the red shift (14 nm) in comparison with emission spectra under excitation wavelengths of 350 and 400 nm, which can be

\* Corresponding author. Tel.: +48 32 2716077. Fax: +48 32 2712969. E-mail: agnieszka.iwan@cmpw-pan.edu.pl.

attributed to a strong correspondence between excitation energy and the vibronic structure of the emission spectra. The DMA solution emission spectrum of doped with 10-camphorsulfonic acid polyketanil PK1 under 400 nm excitation wavelength was red-shifted from the corresponding undoped polymer.<sup>14</sup> Also we discussed the results obtained by Fourier transform infrared (FTIR) spectroscopy after adding of methanesulfonic (MSA) and 10-camphorsulfonic (CSA) acid to polymers in the 1:1, 2:1, and 3:1 ratio with respect to nitrogen in order to ensure full protonation of the polymers. We showed that as in the case of CSA as MSA the spectra were changed mainly in the region characteristic of stretching vibrations of the phenanthridine ring, which indicates that hydrogen from chosen acids interacts with nitrogen present in the phenanthridine ring. For this reason in this paper we investigated how other protonation agents (dopants), i.e., *n*-decyl sulfonic acid (DSA), decanoic acid (DCA), *n*-decyl alcohol (DA), and 1,10-dibromodecane (DBr), i.e., the compounds of similar structure differing in the electronegativity (dipole moments) of the active groups, interacts with nitrogen atom in the phenanthridine ring.

As it was said previously, the halogen bonding has received increasing attention recently. However, particular attention has been focused on the interaction between haloperfluorocarbons and aromatic dinitrogen hydrocarbons<sup>16,17</sup> and between organic nitriles and halogen atoms.<sup>18,19</sup> On the other hand, studies on the nitrogen–halogen interactions involving N-rich heterocycles are relatively rare.<sup>5–8,20,21</sup> The halogen bonding in the papers usually was studied by X-ray diffraction, FTIR, and theoretical calculations.<sup>5–8,20,21</sup> Additionally, we did not find papers where aliphatic halogens will be used as a dopant.

This paper reports the first example of the use of halogen bonding for investigation of the interaction of a halogen compound with polyketimine. A striking parallel is demonstrated between the properties of the halogen and their hydrogen analogues, especially for FTIR and UV–vis spectra of the polyketimine investigated in this paper. Also, interactions between dopant and polymer by wide-angle X-ray diffraction, atomic force microscopy (AFM), and preliminary calculations were studied.

To the best of our knowledge it is the first paper where similarities and differences between undoped and doped polyketimine containing 3,8-diamino-6-phenylphenanthridine and ethylene linkage in the main chain with long-chain aliphatic dopants with different acidities such as DSA, DCA, DA, and DBr are investigated.

## 2. Experimental Section

**2.1. Materials.** DCA (Aldrich), DA (Reachim), DBr (Aldrich), and *N,N*-dimethylacetamide (DMA) were used as received. DSA was prepared according to the method described in ref 15.

**2.1.1. Polyketimine.** The aromatic polyketimine containing the vinylene group and 3,8-diamino-6-phenylphenanthridine in the main chain, namely, the fully conjugated polyketimine, abbreviated in the text as PK1 (see Figure 1), was prepared using the method described previously.<sup>14</sup> Macromolecular parameters and spectroscopic and thermal data of the prepared PK1 are listed below:<sup>14</sup>

PK1: yield (83%). Anal. Calcd for C<sub>35</sub>H<sub>23</sub>N<sub>3</sub> (%): C, 86.60; H, 4.74; N, 8.66. Found: C, 85.79; H, 5.09; N, 8.90.  $\nu_{\max}$  (KBr)/cm<sup>-1</sup>: see Table 1. <sup>13</sup>C NMR (TMS)/(ppm): 112.51, 117.53, 120.91, 121.86, 123.50 (–C=C–), 127.04, 127.84, 127.89, 127.99, 128.82, 128.92, 129.06, 129.26, 129.47, 130.06, 131.12, 133.58, 136.52, 140.17, 146.72, 154.28, 158.12 (C=N in

phenanthridine ring), 161.52 (C=N). UV–vis in DMA:  $\lambda_{\max}$  at 284 and 410 nm. Photoluminescence (PL) in DMA:  $\lambda_{\max}$  at 511 nm (excitation 400 nm). UV–vis in chloroform:  $\lambda_{\max}$  at 280 and 403 nm. PL in chloroform:  $\lambda_{\max}$  at 490 nm (excitation 400 nm). UV–vis in NMP:  $\lambda_{\max}$  at 284 and 413 nm. PL in NMP:  $\lambda_{\max}$  at 505 nm (excitation 400 nm). UV–vis in benzyl alcohol:  $\lambda_{\max}$  at 420 nm. PL in benzyl alcohol:  $\lambda_{\max}$  at 495 nm (excitation 400 nm). UV–vis in *m*-cresol:  $\lambda_{\max}$  at 424 nm. PL in *m*-cresol:  $\lambda_{\max}$  at 591 nm (excitation 400 nm). *T<sub>g</sub>*, 200 °C (473 K).

**2.1.2. Protonation of Polyketimine.** Protonation of PK1 with protonation agent (dopant) was carried out at room temperature using DMA as a solvent. Dopant was added to the DMA solution of polyketimine studied in the 1:1 ratio with respect to nitrogen in the phenanthridine ring (see Figure 1).

**2.2. Characterization Techniques.** Infrared spectra were acquired on a DIGILAB FTS-40A Fourier transform infrared spectrometer in the range of 4000–400 cm<sup>-1</sup> at a resolution of 2 cm<sup>-1</sup> and for an accumulated 32 scans. Samples were analyzed as a pellet in potassium bromide. To compute particular peaks in the region of 1650–1510 cm<sup>-1</sup> a WIN IR curve-fitting program was used choosing an interactive procedure and Gaussian–Lorentzian fitting of curves.

UV–vis absorption spectra were recorded using a Hewlett-Packard 8452A spectrophotometer.

The surface morphology investigations of the undoped and doped polymer cast from DMA solution on the glass were performed in air using a commercial TopoMetrix Explorer AFM in the contact mode.

X-ray diffraction patterns were recorded using powder or film samples on a wide-angle HZG-4 diffractometer working in typical Bragg geometry. Cu K $\alpha$  radiation was applied.

## 3. Results and Discussion

The fully conjugated polyketimine containing the vinylene group and 3,8-diamino-6-phenylphenanthridine in the main chain (PK1) can be dissolved in such solvents as *m*-cresol, benzyl alcohol, DMA, NMP, or chloroform. Good optical quality films can be obtained by casting from solution on glass, quartz, or any other suitable support; however, free foils are brittle. A molecular structure of the PK1 was confirmed by FTIR, <sup>13</sup>C NMR, and elemental analysis<sup>14</sup> (see the Experimental Section).

In this paper we investigate the behavior of PK1 after adding as protonation agents (dopants) DSA, DCA, DA, and DBr, i.e., the compounds of similar structure differing in the electronegativity (dipole moments) of the active groups.

Spectroscopic data discussed below clearly indicate that dopants more or less strongly interact with the polymer chain modifying its conformation toward higher planarity, possibly by protonation, hydrogen, or halogen bonding as schematically depicted in Figure 1. We have studied this problem in greater detail using FTIR, UV–vis spectroscopy, and also by using wide-angle X-ray diffraction and AFM. Results of them we present below.

**3.1. FTIR Investigations. 3.1.1. FTIR Spectrum of Undoped PK1.** The FTIR spectrum of PK1 exhibits the vibration band of the ketimine unit at 1618 cm<sup>-1</sup>, providing further confirmation that the synthesized polymer is the polyketimine. In addition to the C=N stretching band, a band at about 1577 cm<sup>-1</sup> can be distinguished ascribed to C=C stretching deformations in the aromatic ring. It can be noticed that in the case of the phenanthridine ring the presence of the nitrogen atom in the aromatic ring causes the appearance of new bands in the FTIR spectrum due to a change in symmetry of the compound

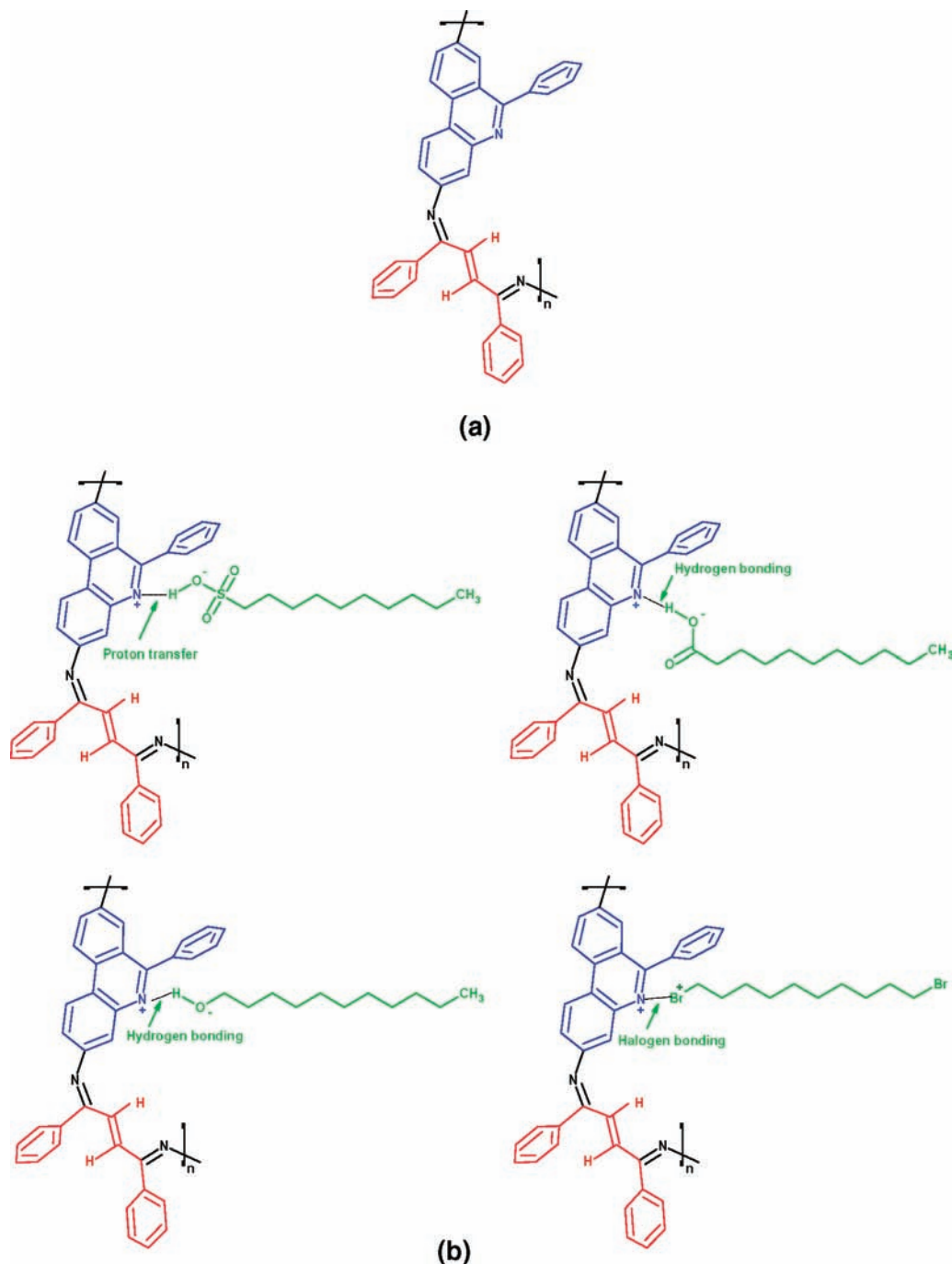


**Figure 1.** Chemical structures of PK1 (a) and proposed schematic model for the interaction between the PK1 and different protonating agents (b).

and also changing in electron charge distribution in the aromatic ring in relation to the phenanthridine ring. It is reflected in our spectra as the appearance of the additional bands at about 1626, 1560, and 1530  $\text{cm}^{-1}$ .<sup>14</sup>

Assignment of particular bands appearing in FTIR spectra of PK1 and DAPP investigated are shown in Table 1.

**3.1.2. FTIR Spectra of Doped PK1.** FTIR spectroscopy provides a facile method of elucidating the effect of Brønsted acid protonation on the molecular structures of the polyketimine. PK1 with different protonating agents (dopants) at 1:1 ratio was dissolved in DMA, and after evaporating of the solvent at vacuum, FTIR spectra were recorded.

FTIR spectra of all the doped samples investigated differ from that of undoped PK1 mostly in the region characteristic for

stretching vibrations of the C=N ketimine group and phenanthridine ring (Figures 2 and 3B–6B). However, it can be noticed that in that region appear also the bands corresponding to stretching vibrations of the phenyl ring. On the other hand the chosen protonating agents have no bands in that region.

The most evident changes are detected for the doped PK1 with DSA. In that case a distinct shoulder at about 1640  $\text{cm}^{-1}$  appeared (Figure 3B), whereas for the other doped samples only the broadening of the band at 1618  $\text{cm}^{-1}$  is recorded.

Thus, in the aim to separate particular bands and compare their areas the curve-fitting calculations were made in that region. The assignment of obtained bands and their areas are shown in the Table 2.

**TABLE 1: Approximate Assignment of IR Bands of PK1 and DAPP Investigated**

assignment	PK1	DAPP
overtone	3650	
$\nu_{as}$ NH <sub>2</sub>	3461	3428
$\nu_s$ NH <sub>2</sub>	3357	3377
$\nu$ NH <sub>2</sub>		3331
$\nu$ NH <sub>2</sub>		3217
$\nu$ CH	3057	3052
$\nu$ CH	3027	
$\delta$ NH <sub>2</sub>		1629
$\nu$ C=C	1701	
$\nu$ C=O	1675	
$\nu$ C=N	1618	1618 sh
$\nu$ Ph	1598	
$\nu$ Pn/ $\nu$ Ph	1577	1577
$\nu$ Pn/ $\nu$ Ph	1564	1564
$\nu$ Pn/ $\nu$ Ph		1540
$\nu$ Ph	1482	1485
$\nu$ Ph	1447	1458 1442
$\nu$ Ph		1442
$\nu$ Ph		1380
$\delta$ CH	1373	1360
	1321	1337
$\delta$ CH		1329
$\omega$ CH	1281	1280
$\delta$ CH <sub>r</sub>	1261	1246
$\delta$ CH <sub>r</sub>	1236	1218
		1202
$\nu$ Ph-N	1179	
$\delta$ CH <sub>mono</sub>		1146
$\delta$ CH <sub>1,3,4</sub>	1074	1072
	1055	
$\delta$ CH <sub>1,3,4</sub>	1027	1030
$\delta$ CH <sub>mono</sub>	1001	1003
$\gamma$ CH <sub>1,3,4</sub>		983
$\gamma$ CH <sub>1,3,4</sub>		900
$\gamma$ CH <sub>1,3,4</sub>		861
$\gamma$ CH		743
$\gamma$ CH <sub>1,3,4</sub>	813	813
$\gamma$ Ph <sub>mono</sub>	789	790
$\gamma$ Ph <sub>1,3,4</sub>	758	761
$\gamma$ Ph <sub>mono</sub>	727	728
$\gamma$ Ph <sub>mono</sub>	698	717 701

As is seen from obtained data for all doped compounds investigated the band at about 1625 cm<sup>-1</sup> ascribed to stretching vibrations of the phenanthridine ring disappears (Table 2).

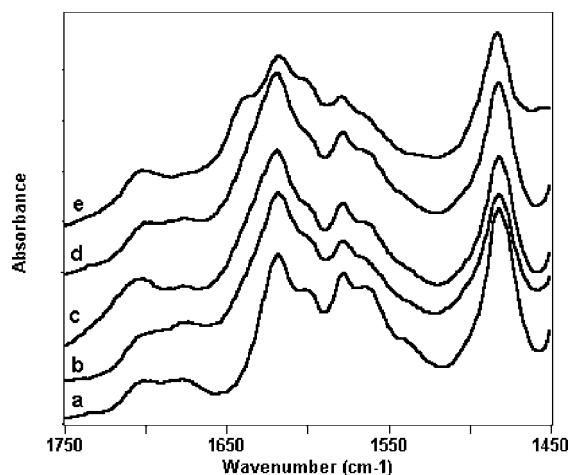


**Figure 2.** FTIR spectra of polyketimine PK1 (a) and 1:1 molar ratio mixtures with DBr (b), DA (c), DCA (d), and DSA (e) in the range of 1750–1450 cm<sup>-1</sup>.

Simultaneously, the other bands corresponding to these vibrations decrease their areas, while the area of the band attributed to the stretching vibrations of the ketimine group diminishes a little. This indicates that protonation agents interact mainly with the nitrogen lone electron pair of the phenanthridine ring. It is in good agreement with our results obtained previously for MSA and CSA.<sup>14</sup> The changes observed depend of the used dopant. For example, we observed a decrease in band intensity of the ketimine group (C=N) after protonation with DSA from 7.14 to 5.86 (see Table 2). In the case of polymer doped with DCA and DA only slight changes can be noticed, whereas for polymer protonated with DBr we have not observed any changes in band intensity due to this group (see Table 2). Moreover, one important detail from the FTIR spectra of protonated PK1 is that in all cases the stretching vibrations of the phenanthridine ring decrease in intensity, also in the case when DBr as a dopant was used (see Table 2). Thus, it was demonstrated that relatively considerable changes as for the bands due to ketimine (C=N) vibrations as for the phenanthridine ring are observed for PK1 doped with DSA. Consequently in that case the biggest area of band arising from stretching vibrations of the C=N<sup>+</sup> group is obtained from curve-fitting calculations. In opposite the less area band due to the C=N<sup>+</sup> group is computed for the PK1 doped with DBr. In that case the area of the band characteristic for the C=N group is almost the same as for the undoped PK1. Relatively small decreasing of the bands due to the phenanthridine ring is observed for the PK1 doped with DCA and DA. In summary, it can be concluded that doping agents investigated causes the shift of the C=N group in the phenanthridine ring to higher wavenumbers as a result of its conjugation of the ionic-bonding system of the polymer chain and dopant systems (see Table 2). After adding DSA to the polyketimine the band characteristic of stretching vibrations of the C=N group in the phenanthridine ring shifts from 1625 to 1640 cm<sup>-1</sup>, whereas for PK1 doped with DA, DCA, and DBr the band characteristic of stretching vibrations of the C=N group in the phenanthridine ring shifts to about 1635 cm<sup>-1</sup> (see Table 2). Decrease in intensity of the ketimine stretching band in the FTIR spectra in the dopant–polyketimine complexes can be rationalized by a redistribution of electron density from the  $\pi$ -electron system of the conjugated polymer.

It can be noticed that the influences observed previously in the case of CSA and MSA are relatively higher than these described above.<sup>14</sup> In summary, it can be concluded that higher interactions between the C=N group in the phenanthridine ring and the protonating agent are observed for the higher-acidity compounds.

On the other hand changes are also observed for the bands corresponding to the stretching vibrations of dopant aliphatic spacers. The bands corresponding to stretching vibrations of the methylene group are conformationally sensitive and can be used to characterize ordering and molecular packing.<sup>22,23</sup> The bands appearing in the region of 2915–2918 cm<sup>-1</sup> corresponding to asymmetric stretching vibrations are attributed to highly ordered aliphatic chains with all-trans conformation, whereas the bands appearing at higher frequencies, i.e., in the region of 2924–2928 cm<sup>-1</sup>, are attributed to gauche conformers. In the case of the compounds investigated by us these bands appear: for “pure” DSA at 2925 and 2910 cm<sup>-1</sup>, for DBr at 2933 and 2919 cm<sup>-1</sup>, for DCA at 2919 cm<sup>-1</sup>, and for DA at 2925 cm<sup>-1</sup>. Thus, it suggests that in the case of DSA and DBr gauche and trans conformations are present, whereas for DCA mainly trans conformers and for DA gauche ones are observed.



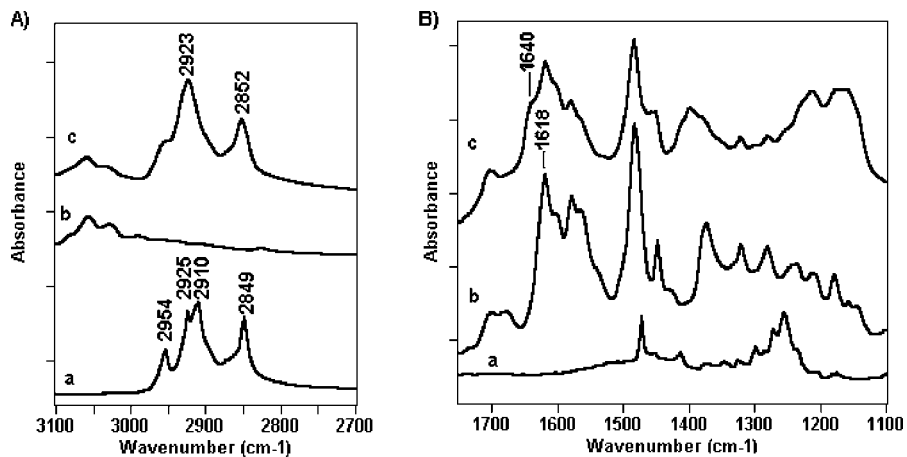


Figure 3. FTIR spectra of DSA (a), PK1 (b), and 1:1 molar ratio of PK1 doped with DSA (c).

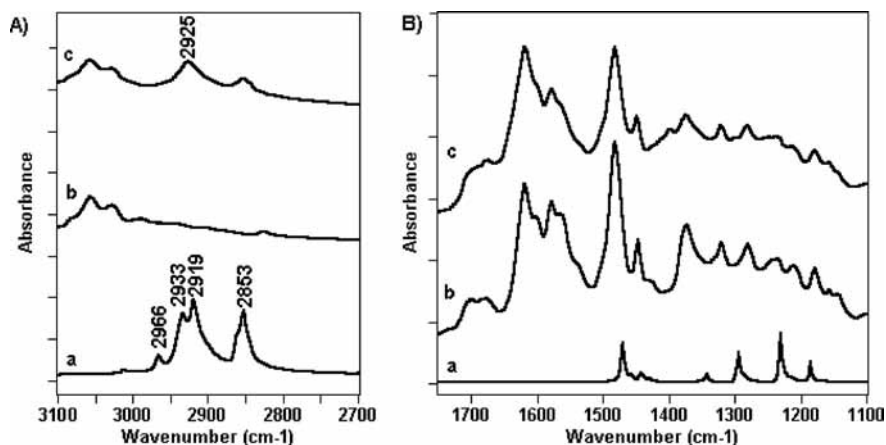


Figure 4. FTIR spectra of DBr (a), PK1 (b), and 1:1 molar ratio of PK1 doped with DBr (c).

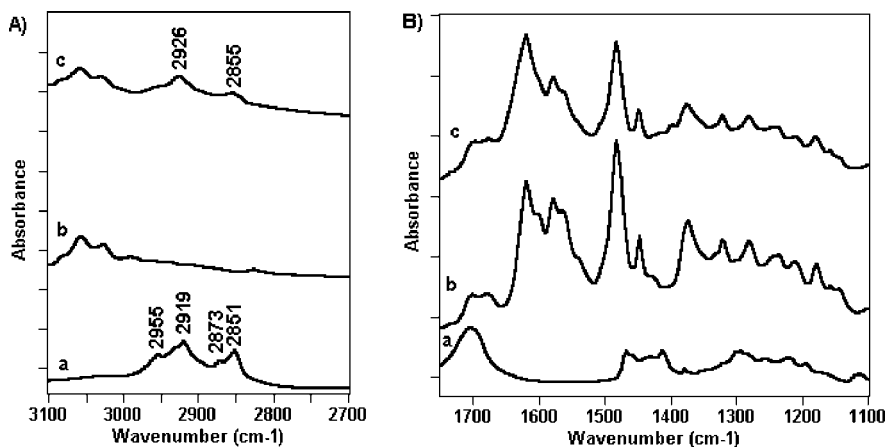


Figure 5. FTIR spectra of DCA (a), PK1 (b), and 1:1 molar ratio of PK1 doped with DCA (c).

Simultaneously, in the region ascribed to symmetric stretching vibrations of the  $\text{CH}_2$  group the band at  $2849$  and  $2853\text{ cm}^{-1}$  for DSA and DBr, respectively, is measured and can be ascribed to vibrations of gauche conformations. In the case of DCA two bands at  $2851$  and  $2873\text{ cm}^{-1}$  and for DA at  $2855$  and  $2877\text{ cm}^{-1}$  are detected which confirms the presence of as gauche as trans conformations in these compounds.

After doping for all the samples investigated only one band as for the asymmetric as for symmetric stretching vibrations appears, i.e., for asymmetric ones at  $2923$ ,  $2925$ ,  $2926$ , and  $2925\text{ cm}^{-1}$  and for symmetric vibrations at  $2852$ ,  $2853$ ,  $2855$ , and  $2854\text{ cm}^{-1}$ , for PK1/DSA, PK1/DBr, PK1/DCA, and PK1/DA,

respectively. Considering literature data these results prove that after doping the aliphatic spacer forms the gauche conformation.

It can be also mentioned that the small-intensity band observed at  $2954$ ,  $2955$ , and  $2956\text{ cm}^{-1}$  for DSA, DCA, and DA is associated with stretching vibrations of the methyl group, whereas that detected for DBr at  $2966\text{ cm}^{-1}$  is attributed to the stretching vibration of methylene in the  $-\text{CH}_2-\text{Br}$  group. These bands are also observed for doped samples.

**3.2. UV-Vis Investigations.** Electronic spectra of the PK1 were detected in DMA solution (concn  $10^{-5}\text{ mol/L}$ ) before and after protonation with DSA, DCA, DA, and DBr. Optical

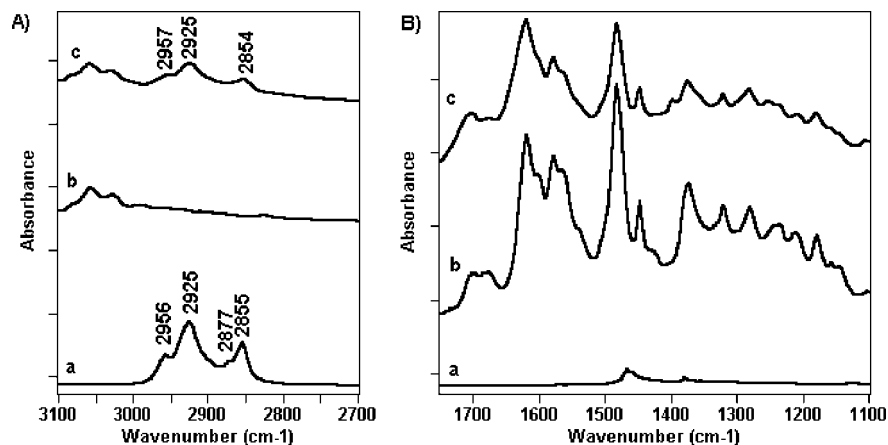


Figure 6. FTIR spectra of DA (a), PK1 (b), and 1:1 molar ratio of PK1 doped with DA (c).

TABLE 2: Results of Curve Fitting of PK1 Doped with DSA, DCA, DA, and DBr in the Region of 1650–1510  $\text{cm}^{-1}$ <sup>a</sup>

sample	area of bands													
	$\nu$ C=N <sup>+</sup>		$\nu$ Phn		$\nu$ C=N		$\nu$ Ph		$\nu$ Ph		$\nu$ Phn			
	wv $\text{cm}^{-1}$	area	wv $\text{cm}^{-1}$	area	wv $\text{cm}^{-1}$	area	wv $\text{cm}^{-1}$	area	wv $\text{cm}^{-1}$	area	wv $\text{cm}^{-1}$	area		
PK1 + DSA	1640	2.51			1618	5.86	1599	3.12	1579	2.74	1564	0.89	1556	1.08
PK1 + DA	1634	2.08			1618	6.79	1598	2.82	1579	1.68	1563	3.42	1539	0.52
PK1 + DCA	1633	2.10			1618	6.71	1597	2.77	1579	1.89	1563	4.01	1540	0.34
PK1 + DBr	1635	1.60			1618	7.12	1598	3.15	1578	1.69	1563	0.93	1556	1.69
PK1			1625	2.57	1618	7.14	1599	6.96	1579	3.35	1562	7.05	1537	2.07

<sup>a</sup>  $\nu$ , stretching vibrations; Phn, phenanthridine ring; Ph, phenyl ring; wv, wavenumber.

properties of PK1 also in solid-state (thin films) and in blend with poly(methyl methacrylate) (PMMA) were investigated.

**3.2.1. UV–Vis Spectrum of PK1.** The absorption spectrum of PK1 in DMA solution is characterized by two bands, one near 284 nm and the other at around 413 nm.<sup>14</sup> The former band can be assigned to the localized absorption of the aromatic ring, whereas the lower-energy band, which is less intense, can be assigned to the charge-transfer band and is characteristic of the ketimine group in the PK1 chain. Figure 7 shows the UV–vis spectra of the undoped and doped PK1 in DMA solution and in blends.

**3.2.2. UV–Vis Spectra of Doped PK1.** The UV–vis spectra of the doped PK1 also provided additional evidence confirming their molecular structure after doping with differing the electronegativity (dipole moments) of the active groups. In the following discussion, the effects of structural modifications will be explored in terms of the effects of doping. The results of the optical absorption measurements of doped PK1 are collected in Table 3.

For the doped polymers in DMA solution changes in the absorption spectra were observed. The charge-transfer band is a little red-shifted, whereas the other band showed a little blue shift (see Table 3 and Figure 7). The second absorption bands are not well-defined and exhibited low intensity (Figure 7). To find the positions of this band the second-derivatives method has been used (i.e., minimum of the second derivative of absorption corresponds to the absorption maximum). The red shift of the charge-transfer band from 413 to about 418 nm indicated the lack of disruption of the conjugated imine band and suggested that the interaction between the nitrogen atom in the phenanthridine ring of PK1 and dopants occurred. The red shift suggests that protonated polymers are more planar than the undoped one. The smallest change of UV–vis spectra was observed for PK1 doped with DCA and DA indicating a weaker interaction between PK1 and DA or DCA caused by the

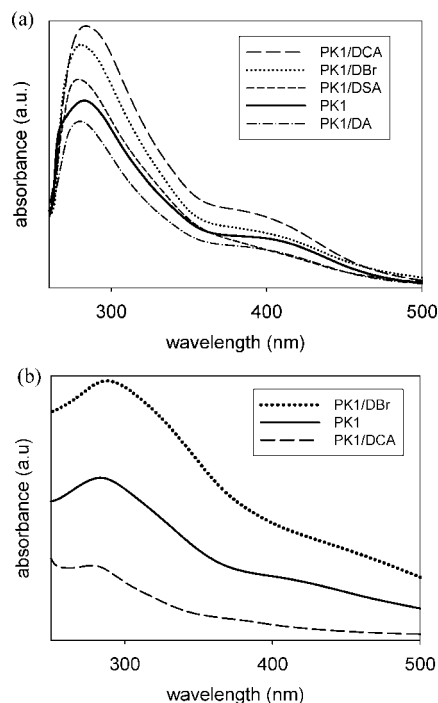


Figure 7. UV–vis spectra of undoped and doped PK1 in DMA (a) and in blends with PMMA (b) (doping level ( $\text{SO}_3\text{H}/\text{C}=\text{N}$  in the phenanthridine ring equal to 1:1)).

differing dipole moment of the active groups and different pH of the dopants. In the case of DA or DCA weaker interaction between the nitrogen atom in the phenanthridine ring was found than in the case of DSA or DBr, which was confirmed also by FTIR spectroscopy. In this case N–HO (PK1/DA) or N–HOOC (PK1/DCA) bonding affects a little the optical properties of PK1 in DMA solution and indicated that in this case  $\pi$ – $\pi$  stacking

**TABLE 3: UV–Vis Parameters of Undoped and Doped PK1 in DMA Solution**

code	$\lambda_1$ [nm]	$\epsilon_1 \times 10^4$ [L/(mol·cm)]	$\lambda_2$ [nm] <sup>a</sup>	$\epsilon_2 \times 10^4$ [L/(mol·cm)]	$E_g$ [eV]
PK1	284	29.43	413	7.10	2.34
PK1/Br	282	38.16	417	7.50	2.22
PK1/DCA	281	41.20	414	9.70	2.33
PK1/DA	280	26.60	415	5.19	2.33
PK1/DSA	278	33.10	418	4.79	2.26

<sup>a</sup>To find the positions of these bands the second-derivatives method has been used.

is the dominant supramolecular interaction. Similar behavior for PK1 doped with *m*-cresol in DMA solution was observed.<sup>14</sup>

The band gaps ( $E_g$ ) of the undoped and doped polymer in DMA solution were obtained from the optical absorption edge, which is a low-energy wing of the lower-energy absorption band. The values of the gaps were significantly dependent on the dopant structure (see Table 3). The difference between the  $E_g$  of the undoped and doped PK1 with DSA was only 0.08 eV, whereas between PK1 and PK1/DBr it was 0.21 eV.

We have also studied the absorption spectra of free transparent foils (blends) obtained by casting a chloroform solution of PK1 and PK1/DBr and PK1/DCA with a nonemissive polymer, PMMA (see Figure 7b). Energy gaps, estimated from absorption spectra, have changed from 2.22 eV for the undoped blend (PK1) to about 2.0 eV for doped polymer foils. As in DMA solution the lowest  $E_g$  was found for PK1 doped with DBr.

Additionally, we measured transmission and fundamental reflectivity in the wide spectral range from 300 to 2500 nm (i.e., 4.13–0.49 eV) for PK1 thin film on the glass substrate. The Kramers–Kronig analysis, applied to reflectance spectra in the low-energy range, yields the value of the refractive index  $n \cong 1.87$ , whereas the thickness of the film ( $d \cong 2.03 \mu\text{m}$ ) was calculated from the interferences of the optical spectra. The energy gap of PK1 thin film (about 2.0 eV) was calculated from the absorption coefficient dependence. The films of doped polymers were not so good quality to obtain their thickness from optical measurements, but their energy gaps were smaller than for undoped PK1 thin film, similarly as for solutions and foils.

A decrease of  $E_g$  value in undoped and doped PK1 was observed in dependence in which form was detected: as a DMA solution, as a blend with PMMA, or as a thin film. The following order was found:  $E_g$  in DMA >  $E_g$  in blend >  $E_g$  in thin film. This is probably due to the more conformational “freedom” of the polymer chains in solution in comparison with the tight packing in the solid state, which can influence conjugation. The differences found in energy gap values along with the maximum electronic absorption bands confirm the differences in planarity and conformations of the polymer chains and as a consequence the different lengths of the conjugated units.

In the discussion of UV–vis spectra of polyconjugated systems one must take into consideration several phenomena such as solvatochromism, thermochromism,<sup>24,25</sup> etc. which are rare in conventional polymers. This is not unexpected since the spectral features are, in this case, very sensitive to even small changes in the chain conformation. Perfectly conjugated polyketimine chain should be planar because planarity assures the best overlap of  $p_z$  orbitals in the  $sp^2$ -hybridized macromolecule, which in turn leads to the smallest band gap between the bands of  $\pi$  orbitals and  $\pi^*$  orbitals. Any conformational change which lowers chain planarity caused either by steric effects or by interactions with the solvents, dopants reduces this overlap, widens the band gap and makes the  $\pi$  and  $\pi^*$  bands narrower.

Thus, in polyconjugated systems any electronic transition associated with the  $\pi$  bonding system must be conformation-dependent. This is also manifested in PK1 after doping (Table 3). A small bathochromic shift in the position of azomethine bands is observed after doping of PK1 in DMA solution. This behavior clearly indicates that dopants are not inert and interact with the polymer chain modifying its conformation toward higher planarity. This can occur via (i) hydrogen-bond formation between phenanthridine-type nitrogens of PK1 which are hydrogen-bonding acceptors and the hydroxyl group of DCA (or DA) which is a good hydrogen-bonding donor, (ii) halogen bond formation between phenanthridine-type nitrogens of PK1 which are hydrogen-bonding acceptors and the halogen group of DBr which is a good halogen-bonding donor, and (iii) protonation of phenanthridine-type nitrogens of PK1 by DSA.

Phenols are much more acidic than aliphatic alcohols ( $pK_a < 10$ ) and in some cases are capable of protonating polymers with basic centers.<sup>26,27</sup>

**3.3. Thin Film Morphology. 3.3.1. AFM Measurements of Undoped and Doped PK1.** The molecular recognition between polyketanil PK1 and protonating agents (DSA, DCA, DA, DBr) using the AFM technique was observed. First we would like to say that the most common method of obtaining contact mode AFM images is the constant force method. In this method the correction voltage for  $z$ -piezo restoring the cantilever to its original deflection is used as the  $z$ -data for imaging the sample surface topography (constant force or topography image). The results of surface topography presented here were obtained in the “constant force” mode. Practically, however, the load force varies during surface scanning, and the cantilever deflection photosensor output so-called “error signal” was used to acquire the error signal image simultaneously with topographical imaging. The error signal images, although containing no true height information, can give additional, complementary information about foil surface appearance and may resemble the micrographs observed in scanning electron microscopy (SEM) or transmission electron microscopy (TEM) images of replicated sample surfaces.

Differences of the unprotonated and protonated PK1 films obtained from DMA solution were found. A thin film of undoped PK1 presents a smooth surface, whereas the film of doped PK1 shows a completely different morphology, with aggregates being more or less clearly visible (Figure 8). Polymeric samples after protonation are showing some organizational features.

Film of PK1 doped with DSA obtained by casting from DMA solution shows a very interesting morphology, characteristic of systems capable of forming organized supramolecular structures (see Figure 8b). Several morphological differences between the undoped and doped PK1 films cast from solvent must be pointed out, and two important conclusions must be drawn from this part of the research. First, it is clear that interactions in the DSA-doped PK1 strongly influence the structural features of the cast films. It is expected that DSA should be a more interacting agent, as compared to DCA or DA, because of its ability to protonate the nitrogen atom in the phenanthridine ring in PK1. Second, it is clear that in DCA the ability to form ordered supramolecular aggregations is retained, whereas in the case of PK1 doped with DA the hydrogen bonds are weak. When PK1 interacts with DBr another type of interaction, namely, halogen bonding is formed. These conclusions are especially important in view of the consecutive studies of the self-organization of dopant–PK1 associations.

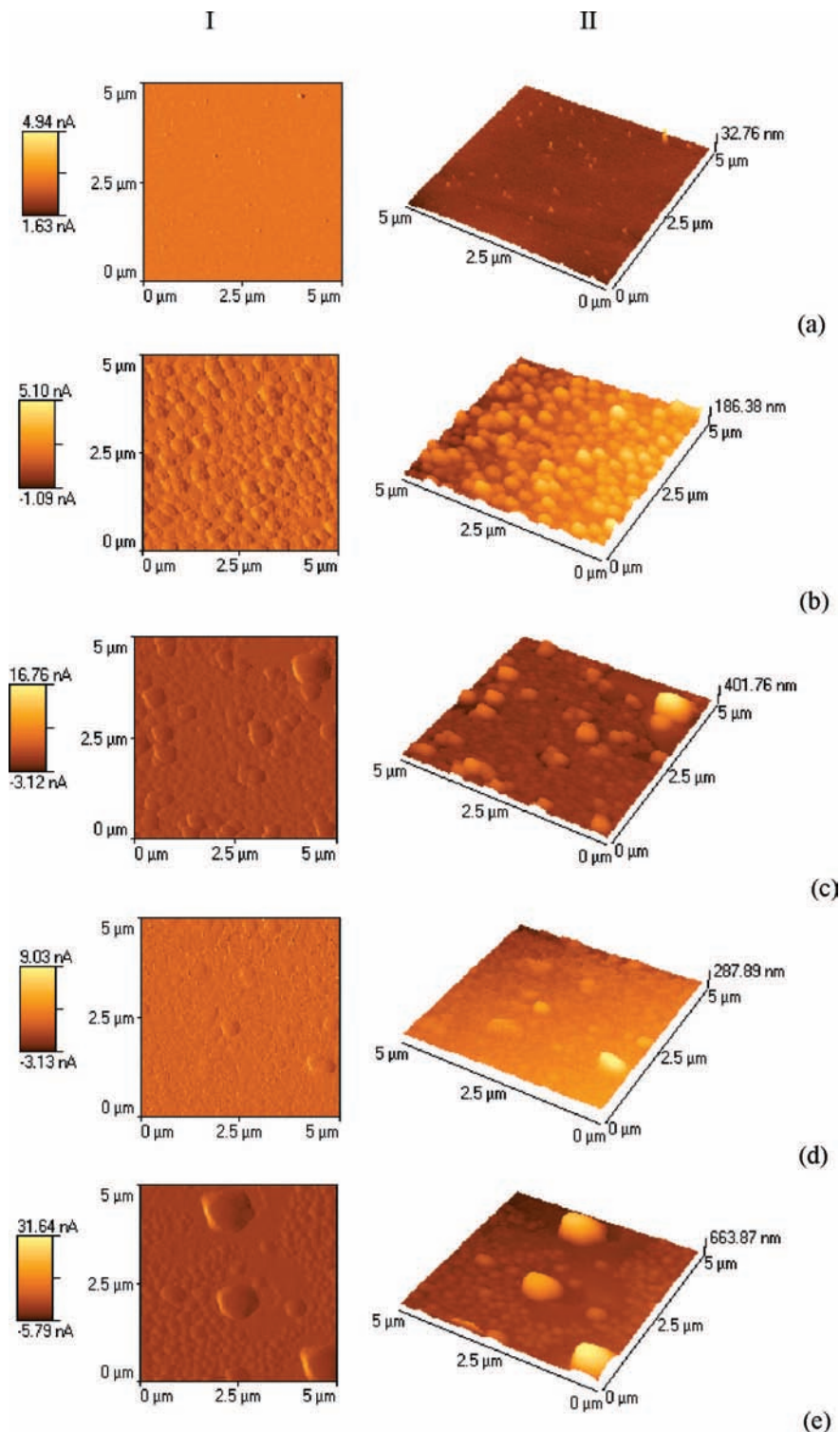


**Figure 8.** AFM images of undoped PK1 (a) and PK1 doped with DSA (b), PK1 doped with DCA (c), PK1 doped with DA (d), and PK1 doped with DBr (e) cast from DMA solution: (I) surface pattern  $5 \times 5 \mu\text{m}^2$ , AFM topography images of compounds, (II) three-dimensional  $5 \times 5 \mu\text{m}^2$ .

**3.4. Wide-Angle X-ray Diffraction.** The WAXD patterns of all the undoped and doped compounds and dopants over the  $2\theta$  range of  $5\text{--}40^\circ$  are shown in Figure 9. PK1 is amorphous as determined by the X-ray diffraction pattern. One broad diffraction peak of diffusion type centered at  $23.28^\circ$  ( $2\theta$ ) was observed in plot presented in Figure 9. The diffraction arising from the crystallites is observed which showed a semicrystalline pattern of doped polymer PK1 with different dopants (Figure 9). The X-ray diffraction pattern of all doped compounds

showed a strong low-angle diffraction peak at about  $31 \text{ \AA}$ , which was close to length of a repeat unit (see Figure 10). Similar behavior for difunctional halogen bonding molecules was observed.<sup>7</sup> Also for doped polymers the broad halo arising from the amorphous region of doped polymers (films cast from DMA) is observed at  $23.16^\circ$  (PK1/DSA),  $23.53^\circ$  (PK1/DCA),  $23.58^\circ$  (PK1/DA), and at  $23.40^\circ$  (PK1/DBr) (Figure 9).

For DSA, DCA, and DBr also WAXD in the solid state as a powder was investigated (see Figure 9). The diffraction arising



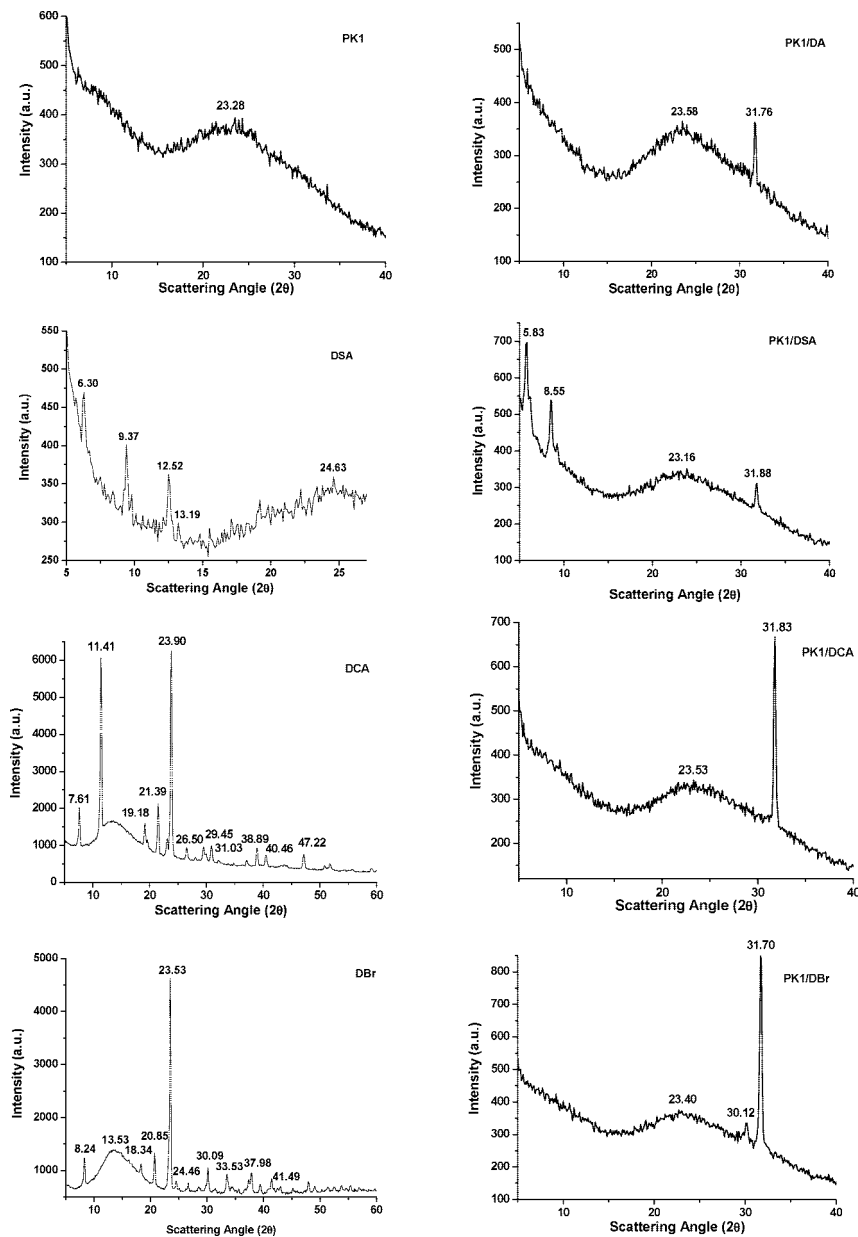


**Figure 9.** WAXD diffractograms intensity vs Bragg angle graph for dopants and undoped and doped PK1.

from the crystallites is observed which showed a crystalline pattern of dopants. The WAXD patterns for dopants show very sharp diffraction peaks with several weak diffractions in smaller angles ( $2\theta$  scanning) and have several peaks, indicating that a highly ordered crystalline structure exists in the dopants. This may be also attributed to the absence of the intermolecular hydrogen bonds in DSA, DCA, and DBr in the solid state. To the contrary, it is clear that in doped polymer the ability to form hierarchically ordered supramolecular aggregations is retained along with the intermolecular hydrogen bonds between dopant and the solvent. This part of our work needs more investigation.

**3.5. Molecular Organization of PK1–Dopant Supramolecules.** Proposed molecular structures for the polyketimine/dopant complex which are considered to be organized in supramolecular structure are presented in Figure 1. Even though the schematic structures of the protonated polyketimine PK1 with different dopants seem similar it is necessary to point out that the distances between the cations located on nitrogen atoms are different (see Table 4) which causes the dopant anions to have different special distances.

As previously explained, the observed changes of spectroscopic properties for the protonated polyketimine can be attributed to the modification of polymer chain planarity, which was proved for polyazomethines.<sup>28</sup> To continue with this idea we would like to make a preliminary geometry optimization (ACD/ChemSketch, 3D Structure Optimization) structure of unprotonated and protonated polyketimine (see Figure 10).

The planarization of the polyketimine takes place and is caused by the protonation of the ketimine group. However, our preliminary geometry optimization shows that the more coplanar structure for PK1/DSA is observed, whereas the more nonplanar structure in PK1 doped with DA and DBr was observed (see Figure 10).

The preliminary calculations of protonated polyketimine PK1 (see Table 4) by using ACD/ChemSketch (3D Structure Optimization) showed that the bond lengths of C=N in the phenanthridine ring in the protonated form are slightly longer than in undoped polymer. Bigger differences were seen in the bond lengths of the nitrogen atom in the phenanthridine ring and the active group of the dopant (see Table 4).

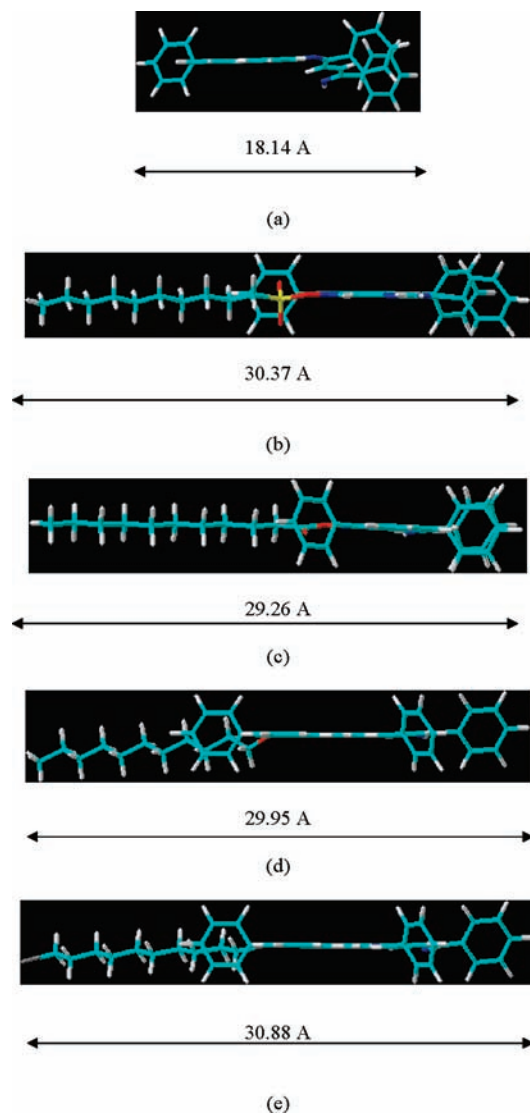


**Figure 10.** Geometry optimization of undoped PK1 (a) and PK1 doped with (b) DSA, (c) DCA, (d) DA, and (e) DBr (side view).

**TABLE 4: Calculated Bond Lengths (angstroms) for Undoped and Doped PK1**

code	bond lengths [angstroms]	
	bonds	distance
PK1	N1–C1	1.3878
PK1/DSA	N1–C1	1.3923
	<b>N1–H1</b>	<b>1.6015</b>
PK1/DCA	N1–C1	1.3924
	<b>N1–H1</b>	<b>1.6129</b>
PK1/DA	N1–C1	1.3944
	<b>N1–H1</b>	<b>1.6061</b>
PK1/DBr	N1–C1	1.3883
	<b>N1–Br1</b>	<b>1.9292</b>

It appears that the N1–H1 bond length in PK1 doped with DSA is the shortest. On the other hand N1–Br1 bond length in PK1 doped with DBr is the largest. Additionally, the bond length of PK1 doped with DCA (N1–H1) is larger than for PK1 doped with DA (N1–H1) (see Table 4). This confirms that protonation changes the geometry of the polyketimine chain. This part of our work needs more investigation.

As said, the halogen bond is highly directional. It in fact occurs along directions which roughly coincide with the axes of the lone pair orbitals in the noncomplexed donor molecule.

The statistical studies in refs 22 and 29 confirmed the directionality of the halogen bond (B–XY, X = halogen, B = donor) in the range of 2.5–3.2 Å for X = Br.<sup>22,29</sup>

Presumably, the hydrogen bonds are much stronger than halogen interactions, and the changes in the properties of polyketimine along with the increase of dopant acidity in the following order should be observed:  $C_{10}H_{22}Br_2 < C_{10}H_{21}OH < C_{10}H_{21}COOH < C_{10}H_{21}SO_3H$ . To confirm or not this scenario we compared relative acidities (pH values) of the studied dopants by using a pH meter. The pH measurements were carried out with a Mettler Toledo SevenMulti pH meter using a glass electrode with KCl. The temperature was maintained at 25 °C. Before experiments calibration of the electrode was done by using the buffers with the following pH: 4.01, 7.00, 9.21, and 11 at 25 °C. The results obtained by using the pH meter are given below. The unexpected pH values order of dopants in DMSO [DSA ( $2.91 \pm 0.05$ ) > DBr ( $7.41 \pm 0.05$ ) > DCA ( $8.29 \pm 0.05$ ) > DA ( $9.42 \pm 0.05$ )] can be explained by the different stability of the ions. This anion stability order is because of the intramolecular hydrogen-bond formation. This behavior is in strong correspondence with preliminary calculations of distance [Å] between the active group of the dopant and the nitrogen atom in the phenanthridine ring (see Table 4). The following three factors may be responsible for the spectacular effect in pH of the dopant structure and consequently in different behavior of doped PK1: (i) the presence of the long aliphatic chain with 10 carbon atoms shifts the value of the pH of DCA and DA to the higher value; it means to the pH 8 or 9, which suggested that these dopants are not acids but weak bases; (ii) DSA as a strong acid dopant transforms the nonplanar conformation of the PK1 into the planar conformation, and in this case the evidence changes in properties were observed; (iii) DBr as a strong base interacts with the nitrogen atom in the phenanthridine ring of the polyketimine and, serving as a key driving force, offers an alternative way to construct supramolecular polymers. This behavior indicates that “the acid motion” of the dopant is the strongest in the case of DSA and is called proton transfer, whereas for weak bases such as DCA and DA a hydrogen bond can be formed. On the other hand when strong base such as DBr was used as a dopant halogen bonding with the nitrogen atom can be created.

When Brønsted acids are used as protonating agent, changes in the properties are due to molecular recognition and formation of supramolecular structures of the polymers chains based on hydrogen or ionic bonding between an acidic type of dopant and basic center in the polymer chain. In this case conformational changes induced by polymer–dopant interactions alter the  $\pi$ -orbital overlap in the polymer chain which results in the energetic change in the electronic transitions. However, efficiency of the acid–base doping may depend not only on the dopant acidity but also on its steric structure and accessibility to the basic center which depends on the polymer chain conformation and the presence of bulky substituents. Another important class of molecular interactions is hydrogen and halogen bonding, which is particularly useful in constructing molecular assemblies.

#### 4. Conclusion

In summary, the present work allows us a better understanding of the role of the halogen and hydrogen bonding and also proton transfer on the formation of self-organized polymers, and this would also help to understand the noncovalent interactions in polyketimines. Apart from the well-known hydrogen bonding, the halogen bonding offers another way to construct supramolecular polymers.

The following conclusions can be drawn from the present work:

1. Four new complexes of polyketimine containing 3,8-diamino-6-phenylphenanthridine and ethylene linkage in the main chain have been obtained and characterized. The complexes were identified by FTIR, UV-vis spectroscopy, WAXD, and AFM.

2. Dopant in association with polyketimine modifies the electronic properties of these compounds and by consequence alters their absorption as an effect of the nitrogen atom in the phenanthridine ring protonation.

3. Doping with dopants changes the FTIR spectra of doped PK1. The biggest changes for PK1 doped with DSA were observed.

4. All of the doped compounds were semicrystalline.

**Acknowledgment.** The authors thank Dr. P. Rannou from CEA in Grenoble, France for the gift sample of DSA.

## References and Notes

- (1) Aizenberg, J. *Adv. Mater.* **2004**, *16*, 1295.
- (2) Lehn, J. M. *Science* **2002**, *295*, 2400.
- (3) Gohlke, H.; Klebe, G. *Angew. Chem., Int. Ed.* **2002**, *41*, 2644.
- (4) Lavigne, J. J.; Anslyn, E. V. *Angew. Chem., Int. Ed.* **2001**, *40*, 3118.
- (5) Lucassen, A. C. B.; Vartanian, M.; Leitus, G.; van der Boom, M. E. *Cryst. Growth Des.* **5** **2005**, 1671.
- (6) Nguyen, H. L.; Horton, P. N.; Hursthouse, M. B.; Legon, A. C.; Bruce, D. W. *J. Am. Chem. Soc.* **2004**, *126*, 16.
- (7) Xu, J.; Liu, X.; Lin, T.; Huang, J.; He, Ch. *Macromolecules* **2005**, *38*, 3554.
- (8) Berski, S.; Ciunik, Z.; Drabent, K.; Latajka, Z.; Panek, J. *J. Phys. Chem. B* **2004**, *108*, 12327.
- (9) Wash, P. L.; Ma, S.; Obst, U.; Rebek, J. *J. Am. Chem. Soc.* **1999**, *121*, 7973.
- (10) Iwan, A.; Sek, D. *Prog. Polym. Sci.* **2008**, *33*, 289.
- (11) Iwan, A.; S k, D.; Kasperczyk, J. *Macromolecules* **2005**, *38*, 4384.
- (12) Iwan, A.; Kaczmarczyk, B.; Kasperczyk, J.; Jurusik, J.; Janeczek, H.; S k, D.; Mazurak, Z. *J. Polym. Sci., Part A: Polym. Chem.* **2006**, *44*, 5645.
- (13) Iwan, A.; Mazurak, Z.; Sek, D. *Polym. Eng. Sci.* **2007**, *47*, 1179.
- (14) Iwan, A.; Mazurak, Z.; Kaczmarczyk, B.; Jarzabek, B.; Sek, D. *Spectrochim. Acta, Part A* **2008**, *69*, 291.
- (15) Iwan, A.; Janeczek, H.; Kwiatkowski, R.; Rannou, P. Manuscript in preparation, 2008.
- (16) Metrangolo, P.; Resnati, G. *Chem. Eur. J.* **2001**, *7*, 2511.
- (17) Corradi, E.; Meille, S. V.; Messina, M. T.; Metrangolo, P.; Resnati, G. *Angew. Chem., Int. Ed.* **2000**, *39*, 1782.
- (18) Lommerse, J. P. M.; Stone, A. J.; Taylor, R.; Allen, F. H. *J. Am. Chem. Soc.* **1996**, *118*, 3108.
- (19) Bond, A. D.; Griffiths, J.; Rawson, J. M.; Hulliger, J. *Chem. Commun.* **2001**, 2488.
- (20) Zhu, S.; Xing, C.; Xu, W.; Jin, G.; Li, Z. *Cryst. Growth Des.* **2004**, *4*, 53.
- (21) Forni, A.; Metrangolo, P.; Pilati, T.; Resnati, G. *Cryst. Growth Des.* **2004**, *4*, 291.
- (22) Jao, T.; Liu, M. *J. Phys. Chem. B* **2005**, *109*, 2532.
- (23) Topaclic, C.; Topaclic, A.; Tesneli, B.; Ricjhardson, T.; Gurol, I.; Ahsen, V. *J. Mol. Struct.* **2005**, *752*, 192.
- (24) Inganas, O. In *Handbook of Organic Conductive Molecules and Polymers, Conducting Polymers*; Nalwa, H. S., Ed.; John Wiley & Sons: New York, 1997; Vol. 3, Chapter 15, p 785.
- (25) Leclerc, M.; Fa d, K. In *Handbook of Conducting Polymers*, 2nd ed.; Skotheim, T. A., Elsembaumer, R. L., Reynolds, J. R., Eds.; Marcel Dekker Inc.: New York, 1998; p 695.
- (26) Kulszewicz-Bajer, I.; Wielgus, I.; Pron, A.; Rannou, P. *Macromolecules* **1997**, *30*, 7091.
- (27) Rannou, P.; Gawlicka, A.; Berner, D.; Pron, A.; Djurado, D. *Macromolecules* **1998**, *31*, 3007.
- (28) Yang, C. J.; Jenekhe, S. A. *Chem. Mater.* **1991**, *3*, 878.
- (29) Lommerse, J. P.M.; Stone, A. J.; Taylor, R.; Allen, F. H. *J. Am. Chem. Soc.* **1996**, *118*, 3108.

JP8019304